Materials Science & Engineering A 627 (2015) 65–71

Contents lists available at ScienceDirect

Materials Science & Engineering A

journal homepage: www.elsevier.com/locate/msea

Influence of crystalline phase volume fraction on the two-way shape memory effect in amorphous–crystalline $Ti_{40.7}Hf_{9.5}Ni_{44.8}Cu_5$ alloy

N. Resnina [a,*], S. Belyaev [a], V. Slesarenko [a], A. Shelyakov [b]

[a] Saint Petersburg State University, Universitetsky pr. 28, Saint Petersburg 198504, Russia
[b] National Research Nuclear University "MEPhI", Kashirskoe sh. 31, Moscow 115409, Russia

ARTICLE INFO

Article history:
Received 6 October 2014
Received in revised form
29 December 2014
Accepted 30 December 2014
Available online 7 January 2015

Keywords:
Shape memory alloys
Amorphous–crystalline alloy
Two-way shape memory effect
Thin ribbons

ABSTRACT

The two-way shape memory effect (TWSME) has been studied in an amorphous–crystalline thin ribbon of $Ti_{40.7}Hf_{9.5}Ni_{44.8}Cu_5$ shape memory alloy with different volume fractions of the crystalline phase. It is found that an increase in the volume fraction of the crystalline phase results in a non-monotonic variation in the value of the TWSME. A maximum strain of 1.1% is observed in the thin ribbon with a 50% crystalline phase. It is found that the TWSME in amorphous–crystalline $Ti_{40.7}Hf_{9.5}Ni_{44.8}Cu_5$ alloy is due to two mechanisms: the formation of high internal stresses on the amorphous/crystalline interfaces due to incompatible strain in amorphous and crystalline phases and the stress caused by defects induced in the crystalline phase during deformation. If the volume fraction of the crystalline phase is 50% or less, then the main contribution to the total TWSME is given by the formation of the internal stresses on the amorphous/crystalline interfaces. In this case, the TWSME value depends on the density of the amorphous/crystalline interfaces, plastic strain and volume fraction of the alloy undergoing a phase transition. If the volume fraction of the crystalline phase is higher than 50%, then the TWSME is due to the formation of the internal stresses on the defects in the crystalline phase and the TWSME value depends on the plastic strain in the crystalline phase and the volume fraction of the crystalline phase.
© 2015 Elsevier B.V. All rights reserved.

1. Introduction

Shape memory alloys demonstrate a unique ability for recovery of large inelastic strain (up to 10%) and generation of high recovery stress up to 1000 MPa [1–2]. This unusual mechanical behaviour is the basis for the wide application of shape memory alloys for space and aircraft engineering [3–7], civil engineering [8–10], medicine [11–14], etc. Recently, a new area for the application of shape memory alloys as active elements in microsystems and microdevices [15–23] has been intensively developing. For instance, the mechanical part of micro-electro-mechanical systems (MEMS) [15–18], microdampers [20] and nanotweezers [22–23] are already produced using the TiNi-based shape memory alloys. In these cases, the size of the shape memory elements should be dozens of microns. To produce such small elements, thin films or ribbons of shape memory alloys are usually used [15–23].

In many applications, the shape memory alloys act as a microactuator. A shape memory actuator may be based on two effects: the one-way shape memory effect or the two-way shape memory effect (TWSME). If the actuator is based on the one-way shape memory effect, then it consists of two parts – a preliminarily deformed shape memory alloy element and a bias elastic element [24]. On heating, the preliminarily deformed shape memory element recovers its strain due to the one-way shape memory effect. As two elements are connected to each other, then a strain recovery in the shape memory element induces a deformation of the bias element and elastic energy is stored in the system. On subsequent cooling, the elastic energy stored in the system induces a deformation of the shape memory element. Therefore, the thermal mechanical actuator changes its sizes or position on heating and cooling. This type of microactuator is used in nanotweezers described in [22–23], where a preliminarily deformed shape memory alloy thin ribbon is connected with a platinum or nickel elastic layer. At the same time, a repeating action of the actuator may be achieved by using the TWSME. In this case, a shape memory alloy demonstrates repeated spontaneous strain variation on cooling and heating without any bias element, and hence, the actuator consists of one part – a shape memory element. According to [2,25], to initiate the TWSME, it is necessary to subject a shape memory alloy to preliminary deformation up to 15–20%. After such a procedure, the TiNi alloy can demonstrate spontaneous deformation of up to 4%.

Actuators using bias elastic elements or TWSME have their advantages and disadvantages. An actuator using the one-way shape memory effect provides a large displacement and force;

* Corresponding author. Tel.: +7 9119949636; fax: +7 8124287079.
E-mail addresses: resnat@mail.ru (N. Resnina), spbelyaev@mail.ru (S. Belyaev), slslesarenko@gmail.com (V. Slesarenko), alex-shel@mail.ru (A. Shelyakov).

http://dx.doi.org/10.1016/j.msea.2014.12.119
0921-5093/© 2015 Elsevier B.V. All rights reserved.

however, it has large dimensions due to the existence of the bias elastic element and it is necessary to solve the problem of the connection of the shape memory element to the elastic element. Meanwhile, the actuator using the TWSME has small dimensions, and it demonstrates no more than 3% of recoverable strain [2].

According to [26], microactuators based on the TWSME are preferable for microdevices due to their small size. The shape memory element is usually produced from a thin ribbon with a thickness of 20–80 μm, and it is deformed by bending or tension. As mentioned above, to achieve a value of TWSME of 4%, it is necessary to subject the ribbons or films to large preliminary strain (15–20%) [2,25]. It is a very difficult procedure due to the small thickness of the samples and the necessity for special and expensive equipment. For instance, to provide a preliminary strain of 15% during bending of the thin ribbon with a thickness of 40 μm, the bending radius should be 133 μm. Such a small bending radius of the sample may be attained using special devices.

In [27–30], the TWSME was found in amorphous–crystalline shape memory thin ribbons. Spontaneous strain was observed on cooling and heating of the ribbon, which consisted of two amorphous and crystalline layers [27–28], without any preliminary deformation or, in the samples consisting of crystalline grains embedded in the amorphous matrix, after small preliminary deformation up to 5–7% [29–30]. In the sample that consisted of two amorphous and crystalline layers, the maximum value of the two-way shape memory effect was 0.4% [27]. At the same time, a value of TWSME of about 1% was found in the amorphous–crystalline samples where crystalline grains were embedded in the amorphous matrix [29–30]. Comparison of the data published in [27–30] shows that the lager TWSME may be observed in amorphous–crystalline alloys with a random distribution of the crystal grain in the amorphous matrix and that the value of TWSME must depend on the volume fraction of the crystalline phase. However, in [29–30], no dependence of the TWSME value on the volume fraction of crystalline phase was found. Moreover, for application of shape memory alloys in microactuators, the stability of the value of the TWSME on repeated thermal cycling is the other important property because it provides constant working parameters of the devices [31]. Thus, to design microactuators based on shape memory alloy thin ribbons, it is necessary to investigate the influence of the volume fraction of the crystalline phase, preliminary deformation and the thermal stability on the TWSME value. Such a study has been carried out in the present work.

2. Materials and methods

An amorphous thin ribbon of the $Ti_{40.7}Hf_{9.5}Ni_{44.8}Cu_5$ alloy obtained by melt spun was used for preparation of amorphous–crystalline samples with different volume fractions of the crystalline phase during partial crystallization at a temperature of 470°C in the differential scanning calorimetry (DSC) apparatus according to the method described in [32]. Using this method, samples with 30%, 40%, 50%, 60%, 70%, 85% and 100% crystalline phase were obtained. The volume fraction of the crystalline phase was calculated as a ratio of heat released during partial crystallization to the heat released during full crystallization. The samples had a length of 5 mm, a width of 1.6 mm and a thickness of 40 μm.

To study the structure of the amorphous–crystalline sample, transmission electron microscopy (TEM) was used in a scanning regime at the Interdisciplinary Resource Centre for Nanotechnology (Saint Petersburg State University) using a Zeiss Libra 200FE TEM (operating at 200 kV). To prepare the sample for TEM, 3-mm diameter plates were cut perpendicularly to the amorphous–crystalline sample surface. The plates were polished by a Precision Ion Polishing System (Gatan PIPS), with an angle of ion beam of 4°, and a voltage of 5 kV at the initial stage of polishing and 1.5 kV at the final stage.

The martensitic transformation in the samples was studied by DSC on cooling and heating in the temperature range of 373 K to 270 K, with a cooling/heating rate of 10 K/min. The temperatures of the martensitic transformation were determined according to the ASTM standard test method F 2004-00.

To study the influence of preliminary deformation on two-way shape memory effect, the procedure described in [29] and consisting of four steps was carried out. In the first step, the amorphous–crystalline sample was deformed by bending between two parallel plates at a constant temperature of 77 K. During the second step, the sample was unloaded, and in the third step it was heated up to 393 K. In the fourth step, the sample was subjected to subsequent cooling and heating in the temperature range of 393 K to 77 K. At each step, photographs of the bent sample profile were taken on the font of scale substrate. The profile of the sample on the image was digitized by ORIGIN software and the bending radius was estimated, which allowed the strain of the sample at each step to be calculated. The strain measured in the first step was the given strain and the strain found in the second step was the residual strain (ε_{res}). The strain measured in the third step was the plastic strain (ε_p). The difference between strain measured during the third and the second steps was the value of the shape memory effect. The difference between the strain measured during the fourth and the third steps was the value of the two-way shape memory effect (ε^{TWSME}).

To study the stability of the TWSME on thermal cycling, two thin ribbons with a volume fraction of the crystalline phase of 50% and 70% preliminarily deformed up to 5.6% and 4.7% of residual strain were subjected to 30 thermal cycles in the temperature range of martensitic transformation (from 393 K to 77 K).

3. Results and discussion

Peculiarities of the crystallization of amorphous TiNi alloys thin ribbons were studied previously [33–38]. It was found that during crystallization spherical grains appeared in the amorphous matrix. Fig. 1 shows the structure of the samples with 40%, 60% and 100% of crystalline phase. All STEM images were analysed and a bimodal lognormal grain size distributions was found. Fig. 2 shows the influence of the volume fraction of the crystalline phase on the average grain sizes determined for both modes of lognormal distribution. It can be seen that an increase in the volume fraction of the crystalline phase leads to an increase in the average grain size and growth in the small grains is slower than that of the large grains.

Martensitic transformations in the amorphous–crystalline sample were studied by DSC. The temperatures of the phase transition as well as the value of heat released on cooling during forward martensitic transformation are given in Table 1. An increase in the volume fraction of the crystalline phase led to an increase in the transformation temperatures and transformation heat and it was due to an increase in the average grain size (Fig. 2). These results are in good agreement with the data published in [32,39–41].

To initiate the two-way shape memory effect, the procedure described in Section 2 was used and the value of the TWSME was measured as the spontaneous strain observed on cooling and heating of the sample preliminarily deformed up to some residual strain. The influences of the preliminary deformation and the volume fraction of the crystalline phase on the one-way shape memory effect have been studied before and published in [29–30]. Fig. 3 shows the dependence of the value of the TWSME (ε^{TWSME})

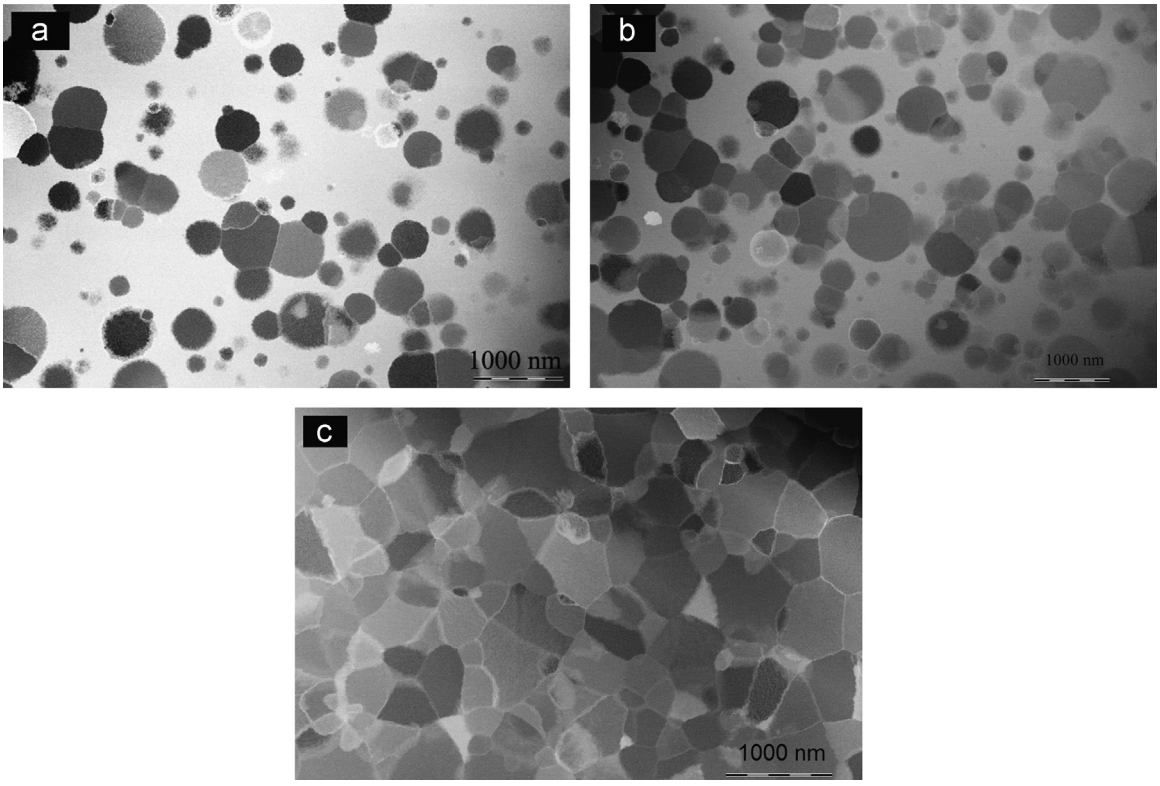


Fig. 1. Transmission electron microscopy in scanning regime images of amorphous–crystalline sample of $Ti_{40.7}Hf_{9.5}Ni_{44.8}Cu_5$ alloys with 40% (a), 60% (b) and 100% (c) crystalline phase.

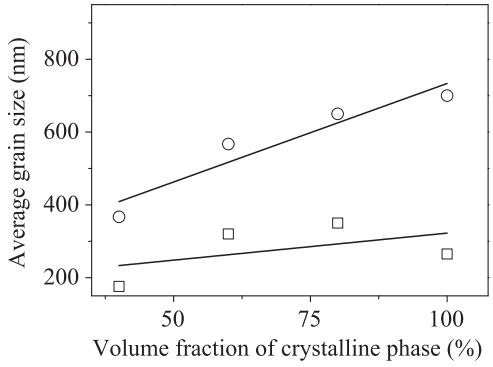


Fig. 2. The dependences of average grain size on the volume fraction of the crystalline phase.

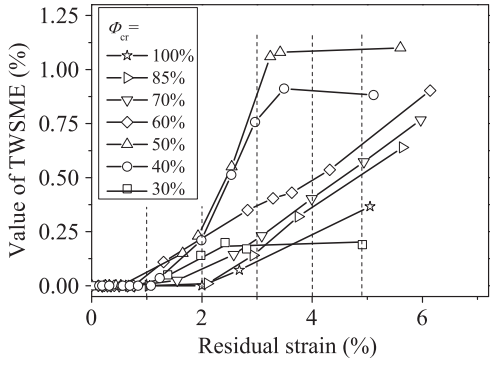


Fig. 3. Dependences of the value of the two-way shape memory effect (TWSME) on the residual strain measured in the sample with different volume fractions of the crystalline phase.

Table 1
Temperatures of martensitic transformations in amorphous–crystalline $Ti_{40.7}Hf_{9.5}Ni_{44.8}Cu_5$ alloy with different volume fraction of crystalline phase. Φ_{cr} – volume fraction of the crystalline phase. M_s, M_f – start and finish temperatures of the forward martensitic transformation; A_s, A_f – start and finish temperatures of the reverse martensitic transformation; E_{fw} – heat released during forward transition.

Φ_{cr}, %	M_s, K	M_f, K	A_s, K	A_f, K	E_{fw}, J/g
0	–	–	–	–	0
30	216	200	270	309	1.15
40	228	220	273	311	2.8
50	241	233	276	312	5.15
60	243	238	277	313	9.4
70	245	241	277	317	11.3
85	258	254	293	319	14.0
100	270	265	307	326	16.7

on residual strain (ε_{res}) obtained in the amorphous–crystalline thin ribbons with different volume fractions of the crystalline phase (Φ_{cr}). The shape of the $\varepsilon^{TWSME}(\varepsilon_{res})$ curves depends on the volume fraction of the crystalline phase. If the volume fraction Φ_{cr} is 50% or less, then an increase in residual strain results in a rise in the value of the TWSME up to saturation. The larger the volume fraction of the crystalline phase, the higher the value of strain saturation. If the volume fraction is larger than 50%, then an increase in residual strain results in an increase in the value of TWSME without saturation. Analysis of the data presented in Fig. 3 shows that, independently of the value of Φ_{cr} there exists a lower limit of residual strain imparted to the sample to observe the TWSME. If the value of residual strain is lesser than the lower limit, the sample is not able to demonstrate the TWSME.

To analyse the influence of the volume fraction of the crystalline phase on the value of the TWSME, the data presented in Fig. 3 have been re-plotted in new coordinates: ε^{TWSME} vs. Φ_{cr}. The value of the TWSME was determined in the samples with different volume fractions of the crystalline phase at a constant residual strain. Five vertical lines were located in Fig. 3 at constant residual

strains: 1%, 2%, 3%, 4% and 4.9% (dashed lines) and the cross-points of these lines and $\varepsilon^{TWSME}(\varepsilon_{res})$ curves were found. The dependences of ε^{TWSME} on the volume fraction of the crystalline phase obtained at constant residual strains are given in Fig. 4. The dependences of $\varepsilon^{TWSME}(\Phi_{cr})$ are non-monotonic and the maximum two-way shape memory value is observed when the volume fraction of the crystalline phase is equal to approximately 45–50%. An increase in residual strain results in an increase in maximum ε^{TWSME}. In the sample pre-strained up to 2% of residual strain, the maximum ε^{TWSME} is equal to 0.27%, and in the sample pre-strained up to 4.9% of the residual strain, the maximum is equal to 1.1%. The values of the TWSME measured in the fully crystalline sample were much lower than the maximum value observed in the sample with a 50% crystalline phase. So, in the fully crystallized sample pre-strained up to 4.9% of the residual strain, the value of the TWSME is equal to 0.34% and it is approximately three times lower than in the sample with a 50% crystalline phase.

Thus, the results given in Fig. 4 show that more preferable conditions for observation of the TWSME exist in the amorphous–crystalline thin ribbons where the volume fraction of the crystalline phase is equal to 45–50%. As shown in Figs. 3 and 4, the TWSME behaviour depends on the volume fraction of crystalline phase and the samples may be divided into two groups. The first group consists of the samples with 50% crystalline phase and in which an increase in Φ_{cr} leads to a rise in TWSME. The second group consists of the samples with a volume fraction of the crystalline phase of more than 50%. In these samples, an increase in Φ_{cr} results in a decrease in the TWSME. Apparently, the difference in the influence of the volume fraction of the crystalline phase on the TWSME is caused by the different mechanisms of TWSME, which is why the thermal stability of the TWSME on thermal cycling has been studied in the samples from these two groups. Fig. 5 shows the dependences of the value of the TWSME on the number of thermal cycles through the temperature range of martensitic transformation observed in the thin ribbons with a 50% crystalline phase (from the first group) and with a 70% crystalline phase (from the second group). Thermal cycling of the sample with a 50% crystalline phase resulted in a very small decrease in the value of TWSME in the first ten cycles. In the first cycle, the value of ε^{TWSME} was equal to 1.1% and in the tenth cycle $\varepsilon^{TWSME}=0.97\%$. Further thermal cycling did not affect the value of the TWSME and in the thirtieth cycle the value of ε^{TWSME} was equal to 0.97%. Thus, one may conclude that the TWSME is stable during thermal cycling of the amorphous–crystalline sample with a 50% crystalline phase. At the same time, thermal cycling of the sample with a 70% crystalline phase through the temperature range of martensitic transformation leads to a monotonic decrease in the value of TWSME. In the first cycle, the value of ε^{TWSME} was equal to 0.5%, in the tenth cycle $\varepsilon^{TWSME}=0.27\%$ and in the thirtieth

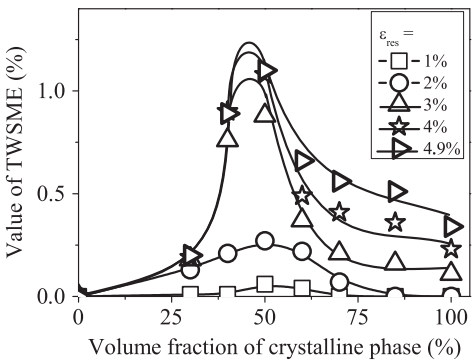


Fig. 4. Dependences of the value of the two-way shape memory effect (TWSME) on the volume fraction of the crystalline phase measured at five constant residual strains: 1%, 2%, 3%, 4% and 4.9%.

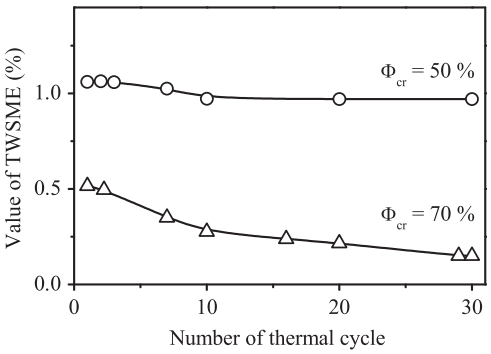


Fig. 5. Dependences of the value of the two-way shape memory effect (TWSME) on the number of thermal cycles measured in the amorphous–crystalline thin ribbons with 50% and 70% crystalline phase preliminarily deformed up to 5.6% and 4.7%, respectively.

cycle the value of ε^{TWSME} was 0.15%. Therefore, the samples from the first group with a volume fraction of the crystalline phase of 50% or less demonstrate a stable TWSME, whereas a degradation of the TWSME is found in the samples from the second group where the Φ_{cr} is more than 50%, as is found for fully crystalline TiNi-based alloys [31].

It is known that the strain variation during the TWSME is caused by the action of the oriented internal stresses that act like external stresses [1]. In fully crystalline TiNi alloys, such oriented internal stresses appear during preliminary deformation due to the formation of defects in the crystalline phase [2]. The formation of defects in the crystalline phase results in a strain recovery on heating is not complete and some plastic strain ε_p remains in the sample. The value of this plastic strain is a measure of internal stresses induce the TWSME, and thus the relation between ε^{TWSME} and ε_p may be given as:

$$\varepsilon^{TWSME} = K\varepsilon_p, \quad (1)$$

where K is the constant [25].

Obviously, in the amorphous–crystalline sample, the value of the two-way shape memory effect should depend on the volume fraction of the crystalline phase because only crystalline grains are able to undergo a martensitic transformation and residual stress appears in the crystalline phase. Hence, the larger the volume fraction of the alloy undergoing a martensitic transformation, the higher the value of the TWSME. Thus, the dependence of ε^{TWSME} on the volume fraction of the crystalline phase may be given as

$$\varepsilon^{TWSME}_{cryst}(\Phi_{cr}) = \varepsilon^{TWSME}_{100\%}\Phi^{tr}, \quad (2)$$

where $\varepsilon^{TWSME}_{100\%}=0.34\%$ is the value of the two-way shape memory effect found in the fully crystalline sample at a residual strain of 4.9%, and Φ^{tr} is the volume fraction of the alloy undergoing martensitic transformation on cooling and heating.

To estimate the volume fraction of the alloy undergoing a phase transformation Φ^{tr}, the ratio of heat released during forward transformation in the samples with different volume fractions of the crystalline phase (Table 1, column 6, lines 1–7) to the heat released during forward transformation in fully crystalline sample (Table 1, column 6, line 8) is found. The dependence of the Φ^{tr} on the volume fraction of the crystalline phase is given in Fig. 6. One could predict that all crystalline grains in the sample undergo a phase transition, thus the Φ^{tr} should be equal to Φ_{cr}. In this case, the dependence between Φ^{tr} and Φ_{cr} should be linear and the linear coefficient must be equal to 1. This linear relationship is shown in Fig. 6 as a dashed line. However, it is seen that the experimental data are located at values lower than the dashed line and the dependence is not linear if the volume fraction of the crystalline phase is less than 60%. It is due to in these amorphous–crystalline

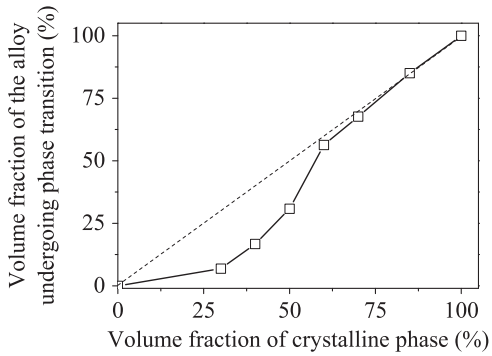


Fig. 6. Dependence of the volume fraction of the alloy undergoing martensitic transformation on the volume fraction of the crystalline phase.

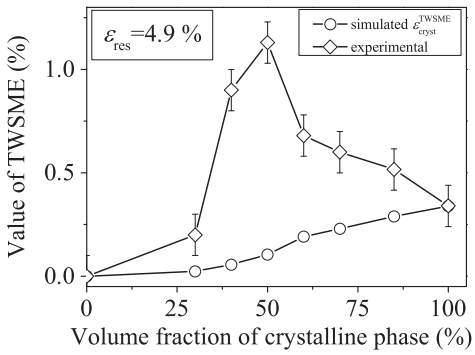


Fig. 7. The $\varepsilon^{TWSME}_{cryst}(\Phi_{cr})$ curve simulated using expression (2) and experimental $\varepsilon^{TWSME}(\Phi_{cr})$ obtained at a residual strain of 4.9% (from Fig. 4).

samples a fraction of the crystal grains with small size is very large and the B2→B19′ transformation does not occur in small grains [39–41]. Hence in the samples with $\Phi_{cr} < 60\%$ some part of the grains do not undergo phase transition that is why the volume fraction of alloy undergoing a phase transformation Φ^{tr} is less than the volume fraction of the crystalline phase. In the samples with 60% and more crystalline phase, most of the crystals undergo a martensitic transformation and the experimental values of Φ^{tr} are equal to Φ_{cr} and $\Phi^{tr}(\Phi_{cr})$ is close to the dashed line.

Using the dependence of $\Phi^{tr}(\Phi_{cr})$ presented in Fig. 6, the $\varepsilon^{TWSME}(\Phi_{cr})$ dependence is estimated through the expression (2) and given in Fig. 7 together with the experimental $\varepsilon^{TWSME}(\Phi_{cr})$ dependence taken from Fig. 4 (a residual strain of 4.9%). It is seen that the simulated curve does not coexist to the experimental curve. This means that the mechanism of the appearance of internal stresses in the crystalline phase during deformation is responsible for the TWSME in the fully crystalline alloy and gives a small contribution to the formation of the TWSME in amorphous–crystalline samples because the simulated data are much lower than the experimental. Hence, it may be concluded that in amorphous–crystalline samples, the additional mechanism for formation of the internal stresses should take place.

In [29], it was suggested that high internal stress might appear at the interfaces between amorphous and crystalline phases. Mechanical properties of amorphous and crystalline phases differ from each other. After preliminary deformation and unloading, a high internal stress appears on the amorphous–crystalline interfaces as a result of a strain incompatibility in amorphous and crystalline phases. These stresses may induce the TWSME on subsequent cooling and heating. Hence, the value of the TWSME should depend on the value of the internal stresses, the density of the amorphous–crystalline interfaces and on the volume fraction of the alloy undergoing a phase transformation. The dependence of $\Phi^{tr}(\Phi_{cr})$ is known (Fig. 6) and thus, it is necessary to find the

Table 2
The values of the residual strain ε_{res}, shape memory effect ε^{SM} and plastic irreversible strain ε_p measured in the amorphous–crystalline samples with different volume fraction of the crystalline phase Φ_{cr}.

Φ_{cr}, %	ε_{res}, %	ε^{SM}, %	ε_p, %
30	4.9	1.5	3.4
40	4.9	2.7	2.2
50	4.9	2.8	2.1
60	4.9	3.8	1.1
70	4.9	4.66	0.24
85	4.9	4.76	0.14
100	4.9	4.76	0.14

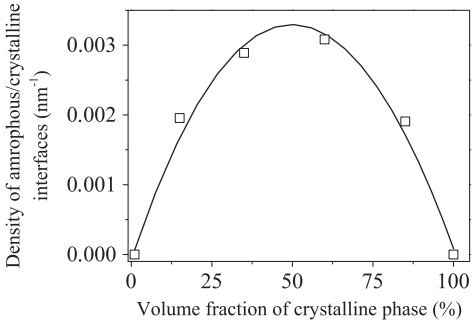


Fig. 8. Dependence of the amorphous/crystalline interfaces density on the volume fraction of the crystalline phase in $Ti_{40.7}Hf_{9.5}Ni_{44.8}Cu_5$ alloy.

dependence of the internal stresses and the density of the amorphous/crystalline interfaces on the volume fraction of the crystalline phase. As mentioned above, a plastic strain may be considered as a measure of internal stress. The value of the plastic irreversible strain was measured as the difference between residual strain (4.9%) and the value of the shape memory effect observed during heating of the samples. In Table 2, it is seen that an increase in Φ_{cr} leads to a significant decrease in plastic irreversible strain.

To calculate the density of the amorphous/crystalline interfaces, the STEM images of the amorphous–crystalline sample structure were analysed, and the length of the amorphous/crystalline interfaces was found. To determine the density of these interfaces per square unit, the value of the total length of the amorphous/crystalline interfaces was divided by the square of the image. Fig. 8 presents the dependence of the density of the amorphous/crystalline interfaces on the volume fraction of the crystalline phase. This curve has a maximum at $\Phi_{cr} \approx 50\%$ and $D_{A/C}(\Phi_{cr})$ dependence may be successfully described by the polynomic equation of the second order:

$$D_{A/C} = A\Phi_{cr}^2 + B\Phi_{cr} + C, \quad (3)$$

where $A = -1.2578 \times 10^{-6}$, $B = 1.25 \times 10^{-4}$, and $C = 1.8142 \times 10^{-4}$.

Therefore, the dependences of the volume fraction of the alloy undergoing a phase transformation, plastic strain and amorphous/crystalline interface density on the volume fraction of the crystalline phase have been found. Thus, the value of the TWSME induced by the internal stresses at the amorphous/crystalline interfaces may be estimated as

$$\varepsilon^{TWSME}_{A/C} = K\varepsilon_p(\Phi_e)\Phi^{tr}(\Phi_{cr})\frac{D_{A/C}(\Phi_{cr})}{D_{max}}, \quad (4)$$

where D_{max} is the maximum value of the amorphous/crystalline interfaces density measured at $\Phi_{cr} \approx 50\%$. The value of the $\varepsilon^{TWSME}_{A/C}$ was calculated according to Eq. (4) for different fractions of the crystalline phase and the $\varepsilon^{TWSME}_{A/C}(\Phi_{cr})$ dependence is given in

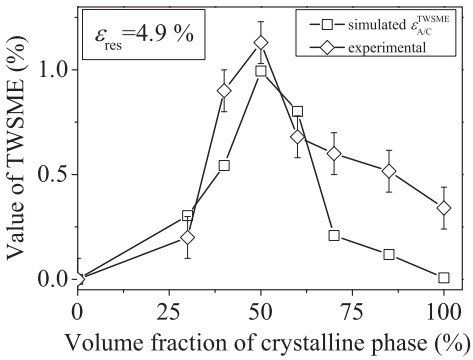


Fig. 9. The $\varepsilon_{A/C}^{TWSME}(\Phi_{cr})$ curve simulated using expression (4) and experimental $\varepsilon^{TWSME}(\Phi_{cr})$ obtained at a residual strain of 4.9% (from Fig. 4).

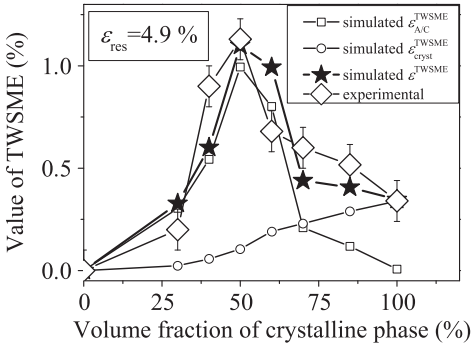


Fig. 10. The $\varepsilon^{TWSME}(\Phi_{cr})$ curve simulated using expression (5), $\varepsilon_{cryst}^{TWSME}(\Phi_{cr})$ curve simulated using the expression (2), $\varepsilon_{A/C}^{TWSME}(\Phi_{cr})$ curve simulated using expression (4) and experimental $\varepsilon^{TWSME}(\Phi_{cr})$ obtained at a residual strain of 4.9% (from Fig. 4).

Fig. 9. The parameter K was fitted to find a good correlation between the theoretical and experimental dependences and was found to be equal to 1.53. The data calculated using Eq. (4) are in good correlation with the experimental data if the volume fraction of the crystalline phase is 60% or less. At the same time, a huge difference between the simulated and experimental results is found at $\Phi_{cr} > 60\%$. It means that the mechanism of internal stresses that appeared at the amorphous/crystalline interfaces is responsible for the TWSME in amorphous–crystalline samples where the volume fraction of the crystalline phase is less than 60%.

As mentioned above, in fully crystalline sample the TWSME is due to a mechanism of oriented internal stress appearance owing to the formation of defects in the crystalline phase (Fig. 7). It is assumed that both mechanisms – formation of the oriented internal stresses in crystalline phase and on the amorphous/crystalline interfaces – are responsible for the TWSME in amorphous–crystalline samples and the total ε^{TWSME} may be found as:

$$\varepsilon^{TWSME}(\Phi_{cr}) = \varepsilon_{cryst}^{TWSME}(\Phi_{cr}) + \varepsilon_{A/C}^{TWSME}(\Phi_{cr}), \quad (5)$$

where $\varepsilon_{A/C}^{TWSME}(\Phi_{cr})$ is calculated according to expression (2) and $\varepsilon_{A/C}^{TWSME}(\Phi_{cr})$ is estimated according to expression (4). The $\varepsilon_{A/C}^{TWSME}(\Phi_{cr})$ dependence has been calculated according to expression (5) and is given in Fig. 10. There is good agreement between the simulated and experimental data. Moreover, it is clear that if the $\Phi_{cr} < 60\%$, then the main contribution to the total TWSME value gives the mechanism of the formation of the internal stresses at the amorphous/crystalline interfaces. If the $\Phi_{cr} > 60\%$, then the TWSME is due to the mechanism of the internal stresses in the crystalline phase, as is observed in the fully crystalline sample.

There is clearly a difference in the strain behaviour on thermal cycling of the amorphous–crystalline samples with a volume fraction of the crystalline phase of 50% or less (the first group of the sample) and more than 50% (the second group of the sample). This is due to a difference in the mechanism inducing the two-way shape memory effect. In the samples with 50% or less of crystalline phase, the TWSME is caused by the appearance of oriented internal stresses on the amorphous/crystalline interfaces due to incompatibility of strains, and the value of this effect depends on the density of the amorphous/crystalline interfaces, plastic strain and volume fraction of the alloy undergoing a phase transition. These parameters do not change during thermal cycling, which is why the value of TWSME remains stable on repeating cooling and heating through the temperature range of the martensitic transformation. In the amorphous–crystalline samples with a volume fraction of the crystalline phase of more than 50%, the main mechanism of TWSME is due to the formation of defects in the crystalline phase. On thermal cycling, the crystalline phase undergoes the martensitic transformations at which the crystalline lattice transforms from one phase to another, and it leads to redistribution of the dislocation structure formed in the sample during preliminary deformation. In this case, a relaxation of oriented stresses induced by crystalline defects occurs and this results in degradation of the TWSME.

4. Conclusions

Amorphous–crystalline thin ribbons of the $Ti_{40.7}Hf_{9.5}Ni_{44.8}Cu_5$ alloy demonstrate the two-way shape memory effect after preliminary deformation. The value of the TWSME is determined by the value of the preliminary strain as well as the volume fraction of the crystalline phase. The dependence of the TWSME value on the volume fraction of the crystalline phase is non-monotonic, and a maximum of 1.1% is observed in the sample with a 50% crystalline phase at 4.9% of residual strain. This value is approximately three times higher than the same value found in the fully crystalline sample.

TWSME behaviour in amorphous–crystalline alloys is caused by two mechanisms: internal stresses induced by defects in the crystalline phase and by the incompatible strain of the amorphous and crystalline phases. If the volume fraction of the crystalline phase is 50% or less, the TWSME is mostly caused by internal stresses that appear at the amorphous/crystalline interfaces. In this case, the TWSME value depends on the density of the amorphous/crystalline interfaces, plastic strain and volume fraction of the alloy undergoing a phase transition. An increase in the volume fraction of the crystalline phase to larger than 50% results in a decrease in the contribution of stresses formed at the amorphous/crystalline interfaces and an increase in the contribution of the stress caused by the defects in the crystalline phase.

Acknowledgements

The study has been carried out through the financial support of Saint Petersburg State University projects (Project Nos. 0.37.177.2014 and 6.37.147.2014) and RFBR project (No. 14-01-31338 mol_a) using the equipment of the Interdisciplinary Resource Centre for Nanotechnology of Saint Petersburg State University. The study of Shelyakov A. was supported by Russian Scientists Found (Project no. 14-22-00098).

References

[1] K. Otsuka, X. Ren, Prog. Mater. Sci. 50 (2005) 511–678.
[2] V. Brailovski, S. Prokoshkin, P. Terriault, F. Trochu, Shape Memory Alloys: Fundamental, Modeling and Applications, Ecole de Technologie Superieure, Quebec, 2003.

[3] A. Razov, A. Cherniavsky, Journal De Physique IV: JP 112 (II) (2003) 1173–1176.
[4] A.I. Razov, Phys. Met. Metall. 97 (2004) S97–S126.
[5] M. Meo, F. Marulo, M. Guida, S. Russo, Compos. Struct. 95 (2013) 756–766.
[6] S. Barbarino, E.L. Saavedra Flores, R.M. Ajaj, I. Dayyani, M.I. Friswell, Smart Mater. Struct. 23 (2014) 063001.
[7] J. Mohd Jani, M. Laery, A. Subic, M.A. Gibson, Mater. Des. 56 (2014) 1078–1113.
[8] A. Isalgue, C. Auguet, G. Careras, V. Torra, Funct. Mater. Lett. 5 (2012) (12500087).
[9] M. Bocciolone, M. Carnevale, A. Collina, N. Lecis, A. Lo Conte, B. Previtali, C.A. Biffi, P. Bassani, A. Tuissi, Frattura ed Integrita Strutturale 23 (2012) 34–46.
[10] W. Raczka, M. Sibielak, J. Kowal, J. Konieczny, J. Low Freq. Noise Vib. Active Control 32 (2013) 117–132.
[11] V. Brailovski, F. Trochu, Bio-Med. Mater. Eng. 6 (1996) 291–298.
[12] T. Yambe, S. Amae, et al., J. Artif. Org. 4 (2001) 88–91.
[13] L.G. Mechado, M.A. Savi, Braz. J. Med. Biol. Res. 36 (2003) 683–691.
[14] G. Li, Y. Zeng, X. Tang, Aust. Phys. Eng. Sci. Med. 33 (2010) 129–136.
[15] R.H. Wolf, A.H. Heuer, J. Microelectromech. Syst. 4 (1995) 206–212.
[16] H. Kahn, M.A. Huff, A.H. Heuer, J. Micromech. Microeng. 8 (1998) 213–221.
[17] Y. Fu, W. Huang, H. Du, X. Huang, J. Tan, X. Gao, Surf. Coat. Technol. 145 (2001) 107–112.
[18] Y. Fu, H. Du, W. Huang, S. Znang, M. Hu, Sens. Actuators A: Phys. 112 (2004) 395–408.
[19] H.J. Zhang, C.J. Qiu, Mater. Sci. Eng. A 438–440 (2006) 1106–1109.
[20] Q. Pan, N. Cho, Sensors 7 (2007) 1887–1900.
[21] Y. Bellouard, Mater. Sci. Eng. A 481–482 (2008) 582–589.
[22] S.P. Belyaev, V.V. Istomin-Kastrovsky, V.V. Koledov, et al., Bull. Russ. Acad. Sci.: Phys. 75 (2011) 1078–1081.
[23] S.P. Belyaev, N.N. Resnina, A.V. Irzhak, et al., J. Alloy. Compd. 586 (2014) S222–S224.
[24] I. Ohkata, Y. Suzuki, in: K. Otsuka, C.M. Wayman (Eds.), Shape Memory Materials, Cambridge University Press, Cambridge, 1998.
[25] Y. Liu, Y. Liu, J. Van Humbeeck, Acta Mater. 47 (1998) 199–209.
[26] K. Mehrabi, M. Bruncko, A.C. Kneissl, J. Alloy. Compd. 526 (2012) 45–52.
[27] A. Shelyakov, N. Sitnikov, S. Saakyan, et al., Mater. Sci. Forum 738–739 (2013) 352–356.
[28] A.V. Shelyakov, N.N. Sitnikov, A.P. Menushenkov, et al., J. Alloy. Compd. 577 (2013) S251–S254.
[29] S. Belyaev, N. Resnina, S. Slesarenko, Smart Mater. Struct. 20 (2011) 082003.
[30] S.P. Belyaev, N.N. Resnina, V.Yu. Slesarenko, A.V. Shelyakov, Inorg. Mater. 2 (2011) 512–516.
[31] H. Scherngell, A.C. Kneissl, Mater. Sci. Eng. A 273–275 (1999) 400–403.
[32] N. Resnina, S. Belyaev, A. Shelyakov, Eur. Phys. J. Spec. Top. 158 (2008) 21–28.
[33] M.J. Vestel, D.S. Grummon, R. Gronsky, A.P. Pisano, Acta Mater. 51 (2003) 5309–5318.
[34] H.-J. Lee, A.G. Ramirez, Appl. Phys. Lett. 85 (2004) 1146–1148.
[35] H.-J. Lee, H. Ni, D.T. Wu, A.G. Ramirez, Appl. Phys. Lett. 87 (2005) 114102 (3 pp.).
[36] X. Wang, J.J. Vlassak, Scr. Mater. 54 (2006) 925–930.
[37] A.G. Ramirez, H. Ni, H.-J. Lee, Mater. Sci. Eng. A 438–440 (2006) 703–709.
[38] K.T. Liu, J.G. Duh, J. Non-Cryst. Solids 353 (2007) 1060–1064.
[39] T. Waitz, H.P. Karnthaler, Acta Mater. 52 (2004) 5461–5469.
[40] T. Waitz, T. Antretter, F.D. Fischer, N.K. Simha, H.P. Karnthaler, J. Mechan. Phys. Solids 55 (2007) 419–444.
[41] T. Waitz, T. Antretter, F.D. Fischer, H.P. Karnthaler, Mater. Sci. Technol. 24 (2008) 934–940.